

## Tunnelling from $\text{Fe}_3\text{O}_4$

This article has been downloaded from IOPscience. Please scroll down to see the full text article.

2001 J. Phys.: Condens. Matter 13 7987

(<http://iopscience.iop.org/0953-8984/13/35/306>)

View [the table of contents for this issue](#), or go to the [journal homepage](#) for more

Download details:

IP Address: 171.66.16.238

The article was downloaded on 17/05/2010 at 04:35

Please note that [terms and conditions apply](#).

# Tunnelling from Fe<sub>3</sub>O<sub>4</sub>

C Sritiwarawong and G A Gehring

Department of Physics and Astronomy, University of Sheffield, Sheffield S3 7RH, UK

E-mail: [php97cs@sheffield.ac.uk](mailto:php97cs@sheffield.ac.uk)

Received 22 March 2001, in final form 11 June 2001

Published 16 August 2001

Online at [stacks.iop.org/JPhysCM/13/7987](http://stacks.iop.org/JPhysCM/13/7987)

## Abstract

Recent experiments on magnetic tunnelling devices based on magnetite film show an unexpectedly low tunnel magnetoresistance despite a high magnetic transition temperature and a high spin polarization of the conduction electrons. The explanation is given in two parts. The first reason for the reduction is the quantum mechanical coupling and relaxation of the conduction electron and core spin. This can reduce the tunnel magnetoresistance substantially. The second is the surface effects in which the magnetic spins at the surface are frustrated as a result of fewer nearest neighbours, surface reconstructions, anti-phase boundaries and the superparamagnetic behaviour. This explains the rapid fall of the magnetization and the tunnel magnetoresistance with temperature.

## 1. Introduction

There has been a recent upsurge in interest in fabricating spin dependent transport devices. One of the material candidates for this kind of device is a transition metal oxide material in which the mobile electrons may be 100% polarized. In order to produce an effective spin dependent device, there are several things to bear in mind. First it should possess a high spin polarization of the conduction electrons, then it should operate at or above room temperature. There are several compounds that are predicted to be ferromagnetic semi-metals, which means that the Fermi surface lies in an energy gap for one spin band. Such materials are CrO<sub>2</sub>, manganite compounds and magnetite (Fe<sub>3</sub>O<sub>4</sub>). CrO<sub>2</sub> and manganite show a very high degree of polarization, 90% and 80% respectively as measured by Andreev reflection [1]. Unfortunately CrO<sub>2</sub> and manganite suffer from a low magnetic transition temperature, which means that they lose a substantial fraction of their conduction electron polarization at room temperature. This causes a sharp drop of magnetoresistance. Magnetite has a very high magnetic transition temperature of around 860 K and is predicted to have a fully polarized conduction band. These properties make magnetite one of the promising candidates for spin-dependent devices.

Magnetite is an inverse spinel ferrite whose formula unit is written as Fe<sub>3</sub>O<sub>4</sub>. There are two types of Fe ion: one is Fe<sup>3+</sup> and the other is Fe<sup>2+</sup> in the ratio of 2:1. There are two different iron sublattices: one is the octahedral (B) site and the other is tetrahedral (A) site

also in a ratio of 2:1. Tetrahedral sites are occupied by  $\text{Fe}^{3+}$  ions while half of the octahedral sites are occupied by  $\text{Fe}^{2+}$  and the other half by  $\text{Fe}^{3+}$  ions. The  $\text{Fe}^{3+}$  ion is a  $3d^5$  high spin ion  $S = 5/2$ . The extra electron on  $\text{Fe}^{2+}$  makes it  $S = 2$ . It is the extra electrons from  $\text{Fe}^{2+}$  ions on the octahedral site that are responsible for the conduction mechanism in this material. The magnetic moments on the A and the B sites are anti-parallel. There are three types of magnetic interaction,  $J_{AA}$ ,  $J_{AB}$  and  $J_{BB}$ , which are the magnetic exchange interaction between A sites, B sites and between A and B sites. In bulk  $\text{Fe}_3\text{O}_4$   $J_{AA} = -11$  K,  $J_{BB} = 3$  K and  $J_{AB} = -22$  K. The strong  $J_{AB}$  plays a crucial role in the magnetic phase. Magnetite under goes a phase transition at 120 K known as the Verwey transition ( $T_v$ ), where the conductivity drops by two orders of magnitude.

As stated above, magnetite shows a promising features for use in spin-polarized devices. However several spin-dependent devices fabricated so far based on magnetite compound such as tunnel junction devices [2, 3] fail to show the expected high degree of spin polarization.

In this paper we examine the polarization expected from the theory and hence the potential of  $\text{Fe}_3\text{O}_4$  for injection devices. Two effects will be considered. We show that at  $T = 0$  a quantum mechanical treatment of the tunnelling from  $\text{Fe}_3\text{O}_4$  demonstrates that the useful polarization may be limited to 67% rather than 100%. At high temperature the polarization of the tunnelling electron from  $\text{Fe}_3\text{O}_4$  will be reduced because of thermally induced disorder at the surface, which is also calculated.

## 2. Tunnelling process in $\text{Fe}_3\text{O}_4$

In this section we consider the transfer process of electrons in two extreme limits and provide the criteria for validation of the two extremes. We derive the expected polarization at  $T = 0$  for two cases of fast and slow hopping. In the slow process the conduction electrons are fully relaxed with the lattice spins while in the fast process the conduction electrons are treated in band theory.

Consider an  $\text{Fe}^{2+}$  ion at time  $t = 0$  such that the transfer of a spin  $|\downarrow\rangle$  has just occurred. The wavefunction is the product of a core spin and an electron in the minority band. It is written as the simple product state

$$\Psi(0) = |\psi_{5/2}\psi_{\downarrow}\rangle \quad (1)$$

where  $\psi_{5/2}$  is the wavefunction for five electrons with parallel spin occupying the  $t_{2g}$  and  $e_g$  states in  $\text{Fe}^{3+}$  ions and  $\psi_{\downarrow}$  is the wavefunction for the added electron. The atomic or fully relaxed state wavefunction is written as

$$\psi_2 = |2, 2\rangle = \sqrt{\frac{5}{6}}|\frac{5}{2}; \frac{5}{2} \downarrow\rangle - \sqrt{\frac{1}{6}}|\frac{5}{2}; \frac{3}{2} \uparrow\rangle \quad (2)$$

where  $\psi_2$  is the wavefunction of six electrons occupying the  $t_{2g}$  and  $e_g$  states. The apparent spin polarization obviously depends on whether the wavefunction is given by equation (1) or equation (2). In the case where band theory is valid (equation (1)) we recover the standard result that the spin polarization is 100% at  $T = 0$  K and the value at higher temperature follows the magnetization. The situation for the fully relaxed state (equation (2)) is more complex and is discussed later in more detail.

We now consider the conditions for the validation of the two extreme cases. The relevant question is whether the added electron has a special wavefunction which is distinct from the core electrons. If the  $\text{Fe}^{2+}$  ion contains six equivalent electrons, it must be in the  $|2, 2\rangle$  state and the process of changing from the  $\text{Fe}^{2+}$  to the  $\text{Fe}^{3+}$  ion may result in the removal of any of the electrons in the  $3d$  shell. This is the extreme tight binding or slow process. In the fast regime it is assumed that the spatial wavefunction of the transferred electron is distinct from

the Fe<sup>3+</sup> ion and hence the spin of the mobile electron will be preserved as it moves through the lattice. Let us write the wavefunction of the core states plus the extra electron in term of the atomic states at time  $t = 0$

$$\Psi(t) = e^{-iE_0t/\hbar} \left[ a\psi_2 + \sum_n b_n \Phi_n \exp\left(-i\frac{(E_n - E_0)t}{\hbar}\right) \right]. \quad (3)$$

The state  $\Phi_n$  is an excited state of the Fe<sup>2+</sup> ion,  $b_n = \langle \Psi(0) | \Phi_n \rangle$  and  $a^2 + \sum_n b_n^2 = 1$ . These excited states are orthogonal to the state  $\psi_2$  i.e.  $\langle \psi_2 | \Phi_n \rangle = 0$ .  $E_0$  and  $E_n$  are the energies of the states  $\psi_2$  and  $\Phi_n$  respectively. These are the atomic energies and hence their difference is of the order of a few electron volts. If the transition occurs after a time  $\tau$  such that  $e^{i\tau(E_n - E_0)/\hbar} \approx 1$  for all states  $n$  such that  $b_n$  is non zero then  $\Psi(\tau) \approx \Psi(0)$  and the band picture is valid. On the other hand if  $\tau$  is such that  $\tau(E_n - E_0) > \hbar$  then the second part of equation (3) will become dephased and not contribute. In this case the slow process in which there is a transfer from state  $\psi_2$  will be valid. Taking  $E_n - E_0 \sim 5$  eV this predicts a critical value of  $\tau$  around  $1.3 \times 10^{-16}$  s. (One might also consider that the slow process is valid if  $a \sim 1$  and  $b_n \sim 0$  but this is really equivalent to the above because we have  $a \sim 1$  only if the hopping energy is very much less than the excitation energies of the ion so that the extreme tight binding holds.)

We have estimated the dwell time for the band and the hopping model. The dwell time for the hopping model is  $\tau = \frac{ne^2 a_o^2}{k_B T \sigma}$ , where  $a_o$ ,  $n$  and  $\sigma$  are the distance between the octahedral sites, density of the electron and conductivity respectively. These values for Fe<sub>3</sub>O<sub>4</sub> are taken from Brabers [4]. At  $T = 300$  K,  $\tau = 3.6 \times 10^{-13}$  s, which is slower than the critical value. On the other hand the dwell time for the band model is  $\tau \approx \frac{\hbar}{w}$  where  $w$  is the bandwidth. The dwell time is  $4.3 \times 10^{-16}$  s, where  $w = 1.55$  eV [5]. This value is comparable with the critical value but the validation of the band model for this material is not clear. In a recent study García *et al* [6] found that the dwell time is less than  $10^{-16}$  s at room temperature: this is the time in which the charge fluctuates between the octahedral sites. This may not be the same as the conduction time, as we propose [7] the dimer model in which one electron is shared between octahedral sites. Therefore there are two time scales associated with the conduction electrons: one is very fast corresponding to the time that each electron spends on each lattice site and the other is slower corresponding to the dwell time for the conduction process. It is the time that is relevant to condition equation (3) so it appears that the slow regime is valid for Fe<sub>3</sub>O<sub>4</sub> particularly at low temperature.

### 3. Slow tunnelling process

In the slow process when a B-site is in the Fe<sup>2+</sup> state we can write it as  $|2, 2\rangle$  as given in equation (2). In the bulk the spin up electron cannot hop to the next nearest neighbour site because it is in state  $|\frac{5}{2}, \frac{5}{2}\rangle$  and it would violate the Pauli exclusion principle. However electrons of either spin can tunnel across a barrier thus the appropriate polarization of Fe<sub>3</sub>O<sub>4</sub> is given by  $P = (\sqrt{5/6})^2 - (\sqrt{1/6})^2 = 2/3$ . However, we note that the final state of the iron ion is different in these two cases. An additional spin wave must be excited for the ion to be left in state  $|5/2, 3/2\rangle$ ; the energy for this comes from the voltage drop between the barriers. There is an interesting difference between the manganite, for which the spin of mobile electrons is parallel to that of the core, and magnetite, for which it is anti-parallel. This spin mixing does not occur if we have parallel coupling.

We now consider a situation in which both electrodes are Fe<sub>3</sub>O<sub>4</sub>. At  $T = 0$  when two electrodes are parallel the sites are in either  $|2, 2\rangle$  or  $|\frac{5}{2}, \frac{5}{2}\rangle$  states and when they are anti-parallel they are in either  $|2, 2\rangle$  or  $|\frac{5}{2}, -\frac{5}{2}\rangle$  states.

We consider first the parallel electrodes such that the sites on the right and left-hand side electrodes are in the  $|\frac{5}{2}, \frac{5}{2}\rangle$  and  $|2, 2\rangle$  states. We can write down the wavefunction as

$$\Psi_1 = |2, 2\rangle^L \otimes |\frac{5}{2}, \frac{5}{2}\rangle^R \quad (4)$$

and consider a process in which an electron is transferred from the left-hand side to the right-hand side across the junction. The only allowed process is that a spin down electron is transferred. After the electron hops to the right hand side the wavefunction becomes

$$\Psi_2 = |\frac{5}{2}, \frac{5}{2}\rangle^L \otimes |2, 2\rangle^R. \quad (5)$$

The probability of tunnelling between state  $|2, 2\rangle$  and state  $|\frac{5}{2}, \frac{5}{2}\rangle$  is given by the square of the transfer matrix element, which is  $M_{2,5/2} = |\langle\Psi_2 T \Psi_1\rangle|^2 = (\sqrt{\frac{5}{6}}\sqrt{\frac{5}{6}})^2 = \frac{25}{36}$ .

We then consider when two electrodes are antiparallel the right and left hand side electrodes are in  $|\frac{5}{2}, -\frac{5}{2}\rangle$  and  $|2, 2\rangle$ . Hence  $\Psi_1 = |2, 2\rangle^L \otimes |\frac{5}{2}, -\frac{5}{2}\rangle^R$ . Here only a spin up electron can hop. As the electron hops the right hand site electrode becomes  $|2, -2\rangle$  state and the left hand side becomes  $|\frac{5}{2}, \frac{3}{2}\rangle$ . The wavefunction is

$$\Psi_2 = |\frac{5}{2}, \frac{3}{2}\rangle^L \otimes |2, -2\rangle^R. \quad (6)$$

The probability of tunnelling is  $M_{2,-5/2} = |\langle\Psi_2 T \Psi_1\rangle|^2 = \frac{5}{36}$ . The tunnelling magnetoresistance (TMR) is given by

$$\frac{M_{\uparrow\uparrow} - M_{\uparrow\downarrow}}{M_{\uparrow\uparrow}} = \frac{M_{2,5/2} - M_{2,-5/2}}{M_{2,5/2}} = 0.80. \quad (7)$$

At a given temperature the  $\text{Fe}^{2+}$  ion can be found in different states according to the  $m_l$  quantum number. It can be in  $|2, \pm 2\rangle$ ,  $|2, \pm 1\rangle$  and  $|2, 0\rangle$  states. The same holds true for the  $\text{Fe}^{3+}$  ion, which can be found in  $|\frac{5}{2}, \pm\frac{5}{2}\rangle$ ,  $|\frac{5}{2}, \pm\frac{3}{2}\rangle$  and  $|\frac{5}{2}, \pm\frac{1}{2}\rangle$  states. The  $|2, 1\rangle$  and  $|2, 0\rangle$  can be written as

$$|2, 1\rangle = \sqrt{\frac{2}{3}}|\frac{5}{2}; \frac{3}{2}\downarrow\rangle - \sqrt{\frac{1}{3}}|\frac{5}{2}; \frac{1}{2}\uparrow\rangle \quad (8)$$

and

$$|2, 0\rangle = \sqrt{\frac{1}{2}}|\frac{5}{2}; \frac{1}{2}\downarrow\rangle - \sqrt{\frac{1}{2}}|\frac{5}{2}; -\frac{1}{2}\uparrow\rangle \quad (9)$$

respectively. The polarizations of the  $|2, \pm 1\rangle$  and  $|2, 0\rangle$  states are  $1/3$  and  $0$  respectively. The average electron spin polarization of the  $\text{Fe}^{2+}$  ion is  $\langle P \rangle = \sum_{m=-2}^{+2} \frac{m_z}{3} P_m = \frac{1}{3}\langle m_l \rangle$ , where  $\langle m_l \rangle$  is the average surface magnetization of an  $\text{Fe}^{2+}$  ion.

We now consider the tunnelling from the  $\text{Fe}^{2+}$  ion to the  $\text{Fe}^{3+}$  ion in the different states of both ions. Using the same method as in  $T = 0$  case we can calculate the tunnelling probability for various states of both  $\text{Fe}^{2+}$  and  $\text{Fe}^{3+}$  ions as summarized in table 1. The transfer of spin up and down electrons between the same Fe ion state is energetically inequivalent; a spin wave is excited in one case but not in the other. For example when an up electron is transferred from state  $|2, 2\rangle$  the core spin will be in state  $|5/2, 3/2\rangle$ , which at low temperature will create a spin wave, while there will be no spin wave excitation if a down electron is transferred. Using table 1 we consider the temperature dependence of the tunnel magnetoresistance. The temperature dependence of the total tunnelling probability from the  $\text{Fe}^{2+}$  ion to  $\text{Fe}^{3+}$  can be written as

$$M_{\uparrow\uparrow(\uparrow\downarrow)}(T) = \sum_{m_i^2=-2}^2 \sum_{m_i^{5/2}=-5/2}^{5/2} M_{m_i^{5/2}}^{m_i^2} P_{m_i^2} P_{\pm m_i^{5/2}} \quad (10)$$

where  $P_{m_l^2}$  and  $P_{m_l^{5/2}}$  are the probability that spin  $S = 2$  and  $S = 5/2$  are in  $m_l^2$  and  $m_l^{5/2}$  states, which is

$$P_{m_l^s} = \frac{e^{\beta m_l^s h}}{Z_S} \quad (11)$$

and  $Z_S$  is a partition function,  $h$  is an effective field and  $\beta$  is  $1/kT$ .

**Table 1.** Tunnelling probability ( $M_{m_l^2, m_l^{5/2}}$ ) between Fe<sup>2+</sup> and Fe<sup>3+</sup> ions for different  $m_l$  quantum number.

$m_l^{S=2}$	$m_l^{S=5/2}$											
	5/2		3/2		1/2		-1/2		-3/2		-5/2	
	↑	↓	↑	↓	↑	↓	↑	↓	↑	↓	↑	↓
2	0	$\frac{25}{36}$	$\frac{1}{36}$	$\frac{5}{9}$	$\frac{1}{18}$	$\frac{5}{12}$	$\frac{1}{12}$	$\frac{5}{18}$	$\frac{1}{9}$	$\frac{5}{36}$	$\frac{5}{36}$	0
1	0	$\frac{5}{9}$	$\frac{1}{18}$	$\frac{4}{9}$	$\frac{1}{9}$	$\frac{1}{3}$	$\frac{1}{6}$	$\frac{2}{9}$	$\frac{2}{9}$	$\frac{1}{9}$	$\frac{5}{18}$	0
-1	0	$\frac{5}{18}$	$\frac{1}{9}$	$\frac{2}{9}$	$\frac{2}{9}$	$\frac{1}{6}$	$\frac{1}{3}$	$\frac{1}{9}$	$\frac{4}{9}$	$\frac{1}{18}$	$\frac{5}{9}$	0
-2	0	$\frac{5}{36}$	$\frac{5}{36}$	$\frac{1}{9}$	$\frac{5}{18}$	$\frac{1}{12}$	$\frac{5}{12}$	$\frac{1}{18}$	$\frac{5}{9}$	$\frac{1}{36}$	$\frac{25}{36}$	0

We consider tunnelling with and without spin wave excitation at low temperature. The tunnelling probability with spin wave excitation is estimated to be

$$M_{\uparrow\uparrow(\uparrow\downarrow)}^{SW} = \frac{(3 - \langle m \rangle_2)(5/2 \mp \langle m \rangle_{5/2})}{36} \quad (12)$$

where plus and minus are for anti-parallel and parallel electrodes respectively. The non-spin-wave tunnelling is estimated to be

$$M_{\uparrow\uparrow(\uparrow\downarrow)}^{NSW} = \frac{(3 + \langle m \rangle_2)(5/2 \pm \langle m \rangle_{5/2})}{36} \quad (13)$$

where plus and minus are for parallel and anti-parallel electrodes respectively. These estimates take into account only  $|2, 2\rangle$  and  $|2, 1\rangle$  states on the left hand side electrode as the probability that this electrode will be in other states is very small. This approximation is valid when the average magnetization is about 90% of the saturated value. In magnetite this approximation is valid up to room temperature. The tunnelling that involves the spin wave is the process that transfers an up electron when the ion is in state  $|2, 2\rangle$  and  $|2, 1\rangle$  and transfers a down electron when it is in state  $|2, -2\rangle$  and  $|2, -1\rangle$ . From equations (12) and (13) it is clear that at  $T = 0$ ,  $\langle m \rangle_{m_l} = m_l$ , when two electrodes are fully parallel, i.e.  $|2, 2\rangle$  and  $|5/2, 5/2\rangle$  states, only non-spin-wave related tunnelling occurs and when they are fully anti-parallel only spin wave related tunnelling occurs. If the spin wave excitations are not allowed due to the small bias voltage the tunnel magnetoresistance is written as

$$\text{TMR}^{\text{NSW}} = \frac{M_{\uparrow\uparrow}^{\text{NSW}} - M_{\uparrow\downarrow}^{\text{NSW}}}{M_{\uparrow\uparrow}^{\text{NSW}}} = \frac{2\langle m \rangle_{5/2}}{\langle m \rangle_{5/2} + 5/2}. \quad (14)$$

As seen from this equation the TMR for the non-spin-wave process is 100% at  $T = 0$ .

If we consider a high bias voltage and assume that the energy difference between the non-spin wave excitation and the spin wave excitation process is very small we may neglect this energy and assume all processes occur equivalently. By summing over all states from table 1 and using the identities  $\langle m \rangle_s = \sum_{m_l^s} m_l^s P_{m_l^s}$  and  $\sum_{m_l^s} P_{m_l^s} = 1$ , the temperature dependence of the tunnelling probability can be written as

$$M_{\uparrow\uparrow(\uparrow\downarrow)}^{\text{NSW}} + M_{\uparrow\uparrow(\uparrow\downarrow)}^{\text{SW}} = M_{\uparrow\uparrow(\uparrow\downarrow)} = \frac{1}{36}(15 \pm \langle m \rangle_2 \langle m \rangle_{5/2}) \quad (15)$$

where plus and minus are for parallel and anti-parallel electrodes. The tunnelling magnetoresistance is

$$\text{TMR} = \frac{M_{\uparrow\uparrow} - M_{\uparrow\downarrow}}{M_{\uparrow\uparrow}} = \frac{4\langle m \rangle_2 \langle m \rangle_{5/2}}{15 + 2\langle m \rangle_2 \langle m \rangle_{5/2}} \quad (16)$$

which is equal to 4/5 or 80% at  $T = 0$  K. If we compare this result with non-spin wave  $\text{TMR}^{\text{NSW}}$  (equation (14)) it is obvious that  $\text{TMR} < \text{TMR}^{\text{NSW}}$ , which shows that spin wave involvement in tunnelling will reduce the TMR substantially.

In other devices such as tunnel junctions fabricated using magnetite and cobalt the tunnelling probability depends on the bias voltage and type of barrier as suggested earlier [8–10]. If d electron filter barriers such as  $\text{SrTiO}_3$  or  $\text{Ce}_{1-x}\text{La}_x\text{O}_{2-x/2}$  are used the TMR from these devices depends strongly on the population of up and down spin electrons in the d band of cobalt. If the tunnelling process involves only the minority d band electrons in cobalt the resistivity for parallel electrodes is lower than the anti-parallel one. This is contrast to the cobalt–insulator–manganite devices for which the resistivity is low when the two electrodes are anti-parallel [8–10]. The differences come from the nature of the spin of the majority electrons in magnetite and manganite. In a manganite-based compound the conduction electrons have spin parallel to the core spin while in magnetite it is antiparallel. When the electrons in the majority d band of cobalt are involved in the tunnelling process the TMR will depend on bias voltage and will decrease and become negative when the electrons in the majority band outnumber those in the minority band. However the negative TMR will not be as large as the positive TMR because there will always be a certain tunnelling of electrons from the minority band. In the case of a barrier in which the s electron in cobalt tunnels predominantly the TMR is positive regardless of the nature of the other electrode [3, 8, 9]. This similarity has not yet been explained but it is suspected that the nature of the interface between cobalt and  $\text{Al}_2\text{O}_3$  is more important than the type of electrode.

In a magnetite–manganite tunnel junction the tunnelling electron will prefer to have spin anti-parallel to the core spin of magnetite and parallel to the core spin of manganite. Therefore in this device the anti-parallel configuration of two electrodes will have a lower resistivity than the parallel one.

#### 4. Surface magnetization

We now consider the reduction which occurs in the ordering at the surface of a magnetite sample as a function of temperature. We consider three main effects that occur which reduce the surface magnetization. First is the reduction in the number of nearest neighbour magnetic atoms which occurs on every surface, secondly the surface reconstruction and distortion of  $\text{Fe}_3\text{O}_4$  and third the anti-phase boundary, which has been observed in magnetite films [11, 12] and will be shown to have a very significant effect on surface magnetization.

These effects are treated using a Monte Carlo technique to simulate the magnetization of both the A and B sites in the cubic phase treated using classical spins. We have simulated both the (100) and (111) surface with and without distortion and also the (100) surface with anti-phase boundaries. We have included more than 6400 sites in the calculation using the standard Metropolis algorithm [13] with the standard random number procedure [14]. The system is simulated using 4000 Monte Carlo steps (MCSs) for stabilizing the system and 3000 MCSs for collecting the data. We defined 1 MCS as the attempt to flip every spin on the system.

The surface of the magnetite film has been studied both in (100) [15] and (111) [16] orientation. We consider first the surface of both (100) and (111) orientations without distortion. The surface of the (100) film is A site terminated with half of the A sites missing and it is A

site terminated in the (111) film. The number of B–B nearest neighbours on the surface is reduced from six to four for (100) and from six to five for the (111) films respectively. The number of B–A nearest neighbours on the surface is also reduced from six to four for the (100) and from six to five for the (111) orientation film. We simulated two configurations, (100) and (111) orientation. In (100) orientation we simulated three different surface conditions, B-site termination, A-site termination and A-site termination with half of the A sites missing while in (111) we simulate in the A-site terminated condition. Figure 1 shows the temperature dependence of reduced surface magnetization without surface distortion.

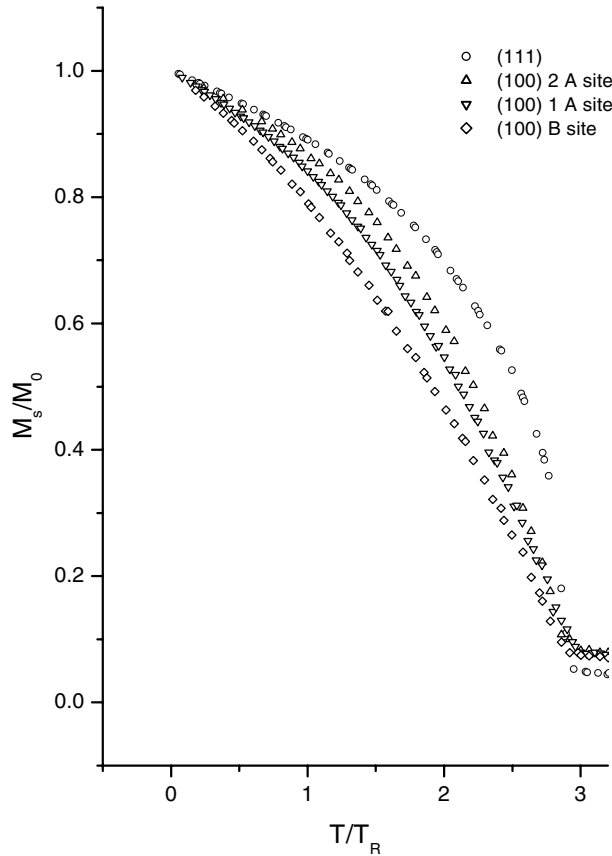


**Figure 1.** Temperature dependence of the reduced surface magnetization for a surface in (111)( $\circ$ ) and (100) orientations. No distortions have been included. The (100) film are simulated in three conditions surface with B-plane termination ( $\diamond$ ), A-plane termination ( $\Delta$ ) and A-plane termination with half of the A sites missing ( $\nabla$ ).  $T_R$  is 300 K.

The surface magnetization of magnetite is very sensitive to any distortion because the magnitude and sign of the interaction  $J_{BB}$  is crucially dependent on the B–O–B bond angle  $\theta$ . For bulk Fe<sub>3</sub>O<sub>4</sub> this angle is 90° and the interaction is weakly ferromagnetic. For a general  $\theta$  we use the well known phenomenological formula for superexchange [17]

$$J_{BB}(\theta) = J_F \sin^2 \theta - |J_{AF}| \cos^2 \theta \quad (17)$$

where  $J_F$  is the ferromagnetic interaction and  $J_{AF}$  is an antiferromagnetic interaction. In magnetite we find that  $|J_{AF}| \gg J_F$ , as shown in table 2. Therefore any small deviation of



B–O–B bond angle away from  $90^\circ$  will have a strong effect on  $J_{BB}$ . In order to take into account the surface reconstructions and distortions, the modified magnetic coupling has to be calculated. We base our calculation on the observed surface distortion of magnetite by Weiss *et al* [16] for the (111) orientation. The modified magnetic interaction can be calculated if the bond angle between magnetic ions and oxygen (Fe–O–Fe) is known. Using equation (17) we can estimate the magnetic interaction for any given bond angle. The bond angle and an estimate  $J_{BB}$  of all cases are summarized in table 2.

**Table 2.** Summary of Fe–O–Fe bond angle and estimated  $J_{BB}$  on different configuration. The  $J_{BB}$  interaction is calculated from the fact that there are two oxygen ions for each Fe pair therefore there are two Fe–O–Fe bond and each contributes  $J_{BB} = 1.5$  K.

Type	Bond angle (deg)			Estimated $J_{BB}$ (K)
	AA	AB	BB	
Bulk	80	125	90	1.5
(100) Anti-phase boundary	80, 110	55, 125	90, 180	1.5, –69.9
(111) with surface distortion	80	125, 130	83, 88, 90, 93, 102	0.4, 1.4, 1.5, 1.3, –1.6

The detail of the observed (111) surface distortion is as follows. The surface relaxation is such that the spacings between layers near the surface are changed. Those layers are oxygen layers, A-site layers and B-site layers. This causes the bond angle between A–O–B and B–O–B to change and this change depends on the position of the A, B and O sites. We have estimated the bond angles according to the observed lattice relaxation and found that the major impact of the lattice relaxation on the bond angle of the Fe–O–Fe bond is on the B-site plane underneath the A-site surface. Every B site on this plane has a total of five B-site nearest neighbours: four of them are in plane and the other is on the plane below. We find that there are two different in-plane B–B interactions on this B plane: one is weak ferromagnetic and the other is weak antiferromagnetic. Therefore every B site on this plane has two in-plane weak antiferromagnetic interactions  $\approx -1.2$  K, two in-plane weak ferromagnetic interactions  $\approx 1.8$  K and one normal ferromagnetic interaction 3 K.

In the (100) film, the surface relaxation has not been reported but the space relaxations such as those observed in (111) film will not affect the bond angle between the B–O–B bonds on the B-site plane because both oxygen ions and B-site ions are on the same plane. However this distortion will affect the A–O–B bond angle but it will not affect  $J_{AB}$  strongly. In the case of a surface with distortion we simulate two different conditions of the (111) film. First all B sites on the surface have two weak antiferromagnetic,  $-1.5$  K and two weak ferromagnetic interactions, 1.5 K. Secondly all B sites on the surface have four strong antiferromagnetic interactions,  $-10$  K. The temperature dependence of the reduced surface magnetization of the (111) film with surface distortion is shown in figure 2.

A magnetite film with an anti-phase boundary has also been investigated. In the previous studies [11, 12] it was found that an anti-phase boundary was responsible for a non-saturated magnetic moment even in a strong magnetic field and possibly shows superparamagnetic behaviour. An anti-phase boundary exists in various ways but can be visualized as a shift by an  $\frac{a_0}{4}$  (110) vector and has a boundary plane given by either {100} or {110} [11, 12]. The effect of an anti-phase boundary on the magnetic interaction is such that the number of bulk A–B bonds is reduced and a strong antiferromagnetic B–B bond across the anti-phase boundary with B–O–B angle equal to  $180^\circ$  is created. The A–O–A bond angle is also increased and several direct exchange bonds between A–A and B–B ions occur [12]. We simulate the anti-phase boundary film with a {100} boundary plane. The condition is that we keep all the interactions

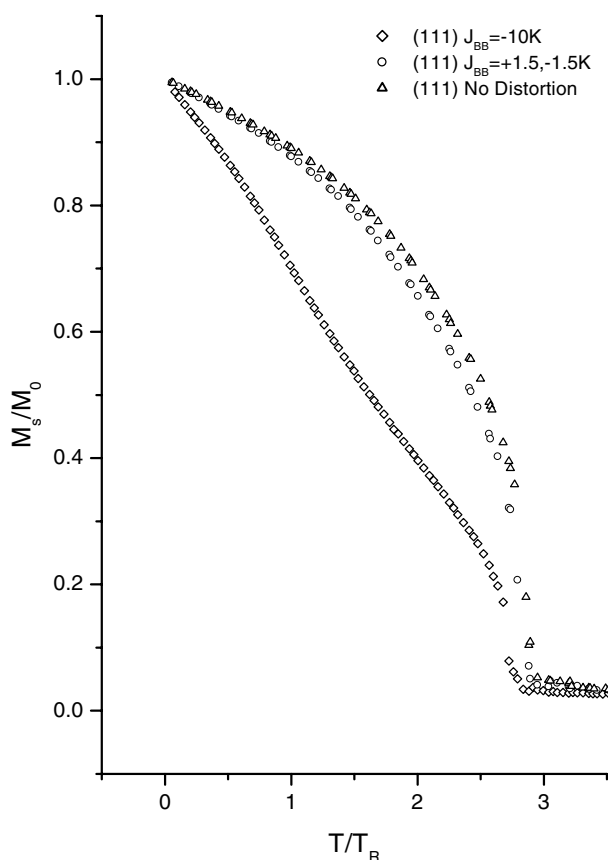


**Figure 2.** Temperature dependence of reduced surface magnetization with surface distortion in the (111) orientation. The film is simulated with two different values of the B–B interaction on the surface,  $J_{BB} = \pm 1.5$  K ( $\circ$ ) and  $-10$  K ( $\diamond$ ) respectively. The (111) surface without distortion is also plotted ( $\Delta$ ).

the same as in the bulk and vary the  $J_{BB}$  of the  $180^\circ$  B–O–B bond angle across the anti-phase boundary. The values of  $J_{BB}$  are  $-10$  K,  $-20$  K and  $-64$  K. The temperature dependence of the reduced surface magnetization of an anti-phase boundary film is shown in figure 3.

## 5. Discussion and conclusion

Table 3 contains a summary of bulk and surface magnetization at room temperature obtained from figures 1, 2 and 3 as well as TMR at room temperature calculated from equation (16). As can be seen from the table that the surface magnetization drops by 10–20% of the bulk value depending on the conditions. It is obvious that the magnetization of a B site on the plane near the surface of Fe<sub>3</sub>O<sub>4</sub>(111) is slightly higher than those of the Fe<sub>3</sub>O<sub>4</sub>(100) surface plane. This is because there will always be an A-site plane above the B-site plane. Also the B-site plane in Fe<sub>3</sub>O<sub>4</sub>(111) has five B-site nearest neighbours rather than four as in Fe<sub>3</sub>O<sub>4</sub>(100).

As mentioned earlier the probability of tunnelling between two magnetite electrodes depends on the surface magnetization of both electrodes. Figure 4 shows the temperature dependence of the tunnelling magnetoresistance between two magnetite electrodes calculated

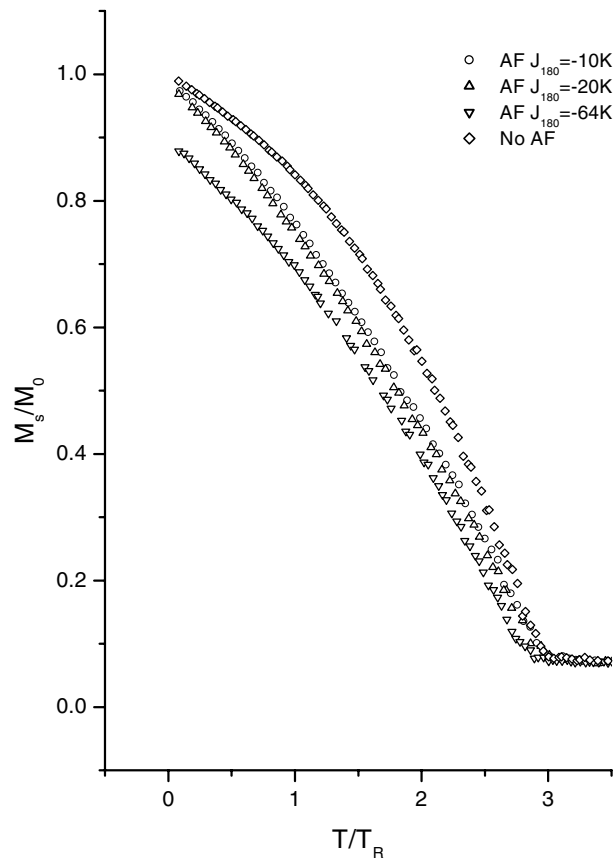


**Figure 3.** Temperature dependence of reduced magnetization in (100) orientation with anti-phase boundary. All anti-phase cases are simulated in the condition that all  $J_{AA}$ ,  $J_{BB}$  and  $J_{AB}$  are bulk values but varying  $J_{180}$ , the  $J_{BB}$  across the anti-phase boundary when the B–O–B bond angle is  $180^\circ$ . The conditions are  $J_{180} = -10$  K ( $\circ$ ),  $-20$  K ( $\triangle$ ) and  $-64$  K ( $\nabla$ ). The (100) film without anti-phase boundary is also plotted ( $\diamond$ ).

**Table 3.** Ratio of surface and bulk magnetization of  $\text{Fe}_3\text{O}_4$  at room temperature. Bulk and surface refer to the ratio of magnetization per site on the B site plane. ‘Bulk’ means that the ratios of magnetization are measured in the plane inside the system while ‘surface’ means the ratios of magnetization on the surface. The value below the distorted (111) film is a value of  $J_{BB}$  near the surface; also the value below the anti-phase (100) film is the  $J_{BB}$  across the anti-phase boundary when the B–O–B bond angle is  $180^\circ$ .

	Without distortion				Distortion		Anti-phase		
	(100) 1-A	(100) 2-A	(100) B	(100) (111)	(111) $\pm 1.5$ K	(111) -10 K	(100) -10 K	(100) -20 K	(100) -64 K
Bulk	0.90	0.90	0.90	0.91	0.91	0.91	0.90	0.89	0.87
Surface	0.84	0.86	0.78	0.89	0.88	0.71	0.77	0.75	0.70
TMR	0.64	0.66	0.57	0.69	0.68	0.50	0.57	0.54	0.49

from equation (16) assuming that the temperature dependence of the average surface magnetization is the same for both spin 2 and 5/2, i.e.  $\frac{\langle m \rangle_2}{2} = \frac{\langle m \rangle_{5/2}}{5/2}$ . The calculations indicate

that the magnetoresistance as high as 50% at room temperature would be expected in the worst cases but experimentally only a few per cent of TMR has been achieved [2, 3]. The reason for such a small TMR has been suggested in terms of the interface effect [2, 3]. However it is also possible that it is caused by the formation of a superparamagnetic region between the anti-phase domain boundaries occupied at the interface [18]. We estimated the temperature at which a superparamagnetic phase would occur between adjacent anti-phase domains is about 100 K. This would have a very strong effect on the TMR.

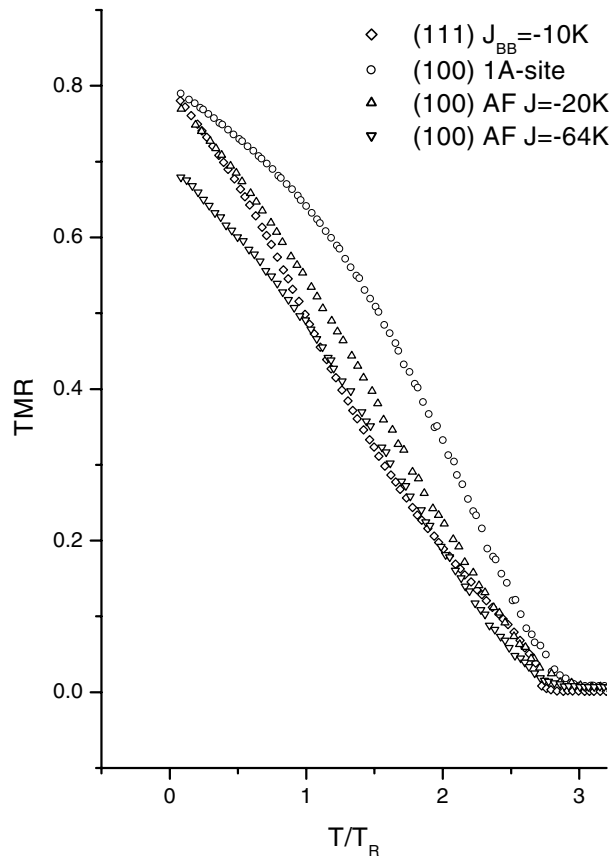


**Figure 4.** Temperature dependence of TMR calculated from equation (16) in the case of (111) orientation with surface distortion  $J_{BB} = -10$  K (◇), (100) A-plane termination with half A sites missing (○) and anti-phase (100) with  $J_{180} = -20$  K (△) and  $-64$  K (▽).

In conclusion we have shown that the tunnelling probabilities between two Fe ion electrodes of spin-dependent devices based on magnetite compounds are lower than expected if the slow process is valid across the junction even in the ground state. Also the presence of spin wave excitation can reduce the TMR. This is a unique feature of magnetite as the mobile electrons couple antiferromagnetically to the core spin. At higher temperature the tunnel magnetoresistance is lowered by the frustration of the surface spins due to distortion at the surface and also the possibility of a superparamagnetic region between the anti-phase boundaries.

## Acknowledgments

The authors would like to thank Rik Tyer for reading the manuscript and one of the authors (CS) would like to thank The Royal Thai Government for financial support.

## References

- [1] Soulen R J Jr *et al* 1999 *J. Appl. Phys.* **85** 4589
- [2] Li X W, Gupta A, Gang Xiao, Qian W and Dravid V P 1998 *Appl. Phys. Lett.* **73** 3282
- [3] Seneor P, Fert A, Maurice J-L, Montaigne F, Petroff F and Vaurès A 1999 *Appl. Phys. Lett.* **74** 4017
- [4] Brabers V A M 1995 *Handbook of Magnetic Materials* vol 8, ed K H J Buschow (Amsterdam: Elsevier) p 189
- [5] Zhang Ze and Satpathy S 1991 *Phys. Rev. B* **44** 13 319
- [6] García J, Subías G, Proietti M G, Renevier H, Joly Y, Hodeau J L, Blasco J, Sánchez M C and Bérrar J F 2000 *Phys. Rev. Lett.* **85** 578
- [7] Gehring G A and Sritiwarawong C 2000 to be published
- [8] Teresa J M D, Barthélémy A, Fert A, Contour J P, Montaigne F and Seneor P 1999 *Science* **286** 507
- [9] Teresa J M D, Barthélémy A, Contour J P and Fert A 2000 *J. Magn. Magn. Mater.* **211** 160
- [10] Teresa J M D, Barthélémy A, Fert A, Contour J P, Lyonnet R, Montaigne F, Seneor P and Vaurès A 1999 *Phys. Rev. Lett.* **82** 4288
- [11] Hibma T, Voogt F C, Niesen L, van der Heijden P A A, de Jonge W J M, Donkers J J T M and van der Zaag P J 1999 *J. Appl. Phys.* **85** 5292
- [12] Margulies D T, Parker F T, Rudee M L, Spada F E, Chapman J N, Aitchison P R and Berkowitz A E 1997 *Phys. Rev. Lett.* **79** 5162
- [13] Binder K and Heermann D W 1988 *Monte Carlo Simulation in Statistical Physics: an Introduction* (Berlin: Springer)
- [14] Press W H, Teukolsky S A, Vetterling W T and Flannery B P 1997 *Numerical Recipes in C* (Cambridge: Cambridge University Press)
- [15] Mijiritskii A V, Langelaar M H and Boerma D O 2000 *J. Magn. Magn. Mater.* **211** 278
- [16] Weiss W, Barbieri A, Van Hove M A and Somorjai G A 1993 *Phys. Rev. Lett.* **71** 1848
- [17] Atanasov M A and Angelov S 1985 *Solid State Commun.* **56** 743
- [18] Voogt F C, Palstra T T M, Niesen L, Rogojuanu O C, James M A and Hibma T 1998 *Phys. Rev. B* **57** R8107